

Effects of Aerosol Particles on the Microphysics of Coastal Stratiform Clouds

CYNTHIA H. TWOHY

*National Center for Atmospheric Research, Boulder, Colorado**

PHILIP A. DURKEE

Naval Postgraduate School, Monterey, California

BARRY J. HUEBERT

University of Hawaii, Honolulu, Hawaii

ROBERT J. CHARLSON

University of Washington, Seattle, Washington

(Manuscript received 6 January 1994, in final form 3 August 1994)

ABSTRACT

Aerosol particles can act as cloud condensation nuclei and thereby influence the number and size of droplets in clouds. Consequently, anthropogenic particles have the potential to influence global climate by increasing cloud albedo and decreasing precipitation efficiencies. Enhanced cloud reflectances associated with increases in particle number have been observed, but our understanding of these interactions has been hindered by incomplete empirical studies and models of limited scope.

In this study, aerosol and droplet size distributions were measured on 13 research flights in stratiform clouds within 300 km west of the northern California coast. The chemical composition of the droplet solute was also assessed. Microphysical and chemical properties indicated that most of the clouds were influenced by pollution from the North American continent, but pristine marine clouds were sampled on one flight during westerly flow conditions. Data from this flight and another, representing a pristine and polluted environment, were compared with high-resolution satellite observations.

In the polluted case, particle and droplet number concentrations decreased, mean droplet size increased, and satellite-derived reflectance at 3.7 μm decreased with increasing distance from the northern California urban region. Relative to the unpolluted stratiform cloud, the polluted cloud had, on average, a sulfate concentration that was higher by an order of magnitude, droplet number concentrations higher by a factor of 6, droplet sizes smaller by a factor of 2, and 3.7- μm reflectance that was higher by a factor of 2. However, no significant difference in the visible reflectance was detected between the two cases, probably a result of differences in liquid water path.

1. Introduction

Clouds are present over about 60% of the earth's surface and play a vital role in atmospheric chemistry and climate. Direct climatic impacts of clouds include reflection of solar radiation, absorption of longwave radiation, and removal of water from the atmosphere as precipitation.

Cloud droplets form in the earth's atmosphere when water vapor condenses onto a suitable particle (cloud

condensation nucleus or CCN). The number of cloud condensation nuclei in pristine environments is usually fewer than 100 cm^{-3} , while in polluted areas CCN populations of 1000 cm^{-3} or more are not uncommon (Twomey and Wojciechowski 1969; Radke and Hobbs 1976). The total liquid water produced in a cloud is determined by thermodynamic processes, but the *distribution* of water to the droplets is primarily influenced by the CCN number concentration. The low number concentrations of CCN in remote marine environments produce clouds with correspondingly low droplet concentrations and therefore large droplet sizes, while continental or polluted clouds tend to have higher concentrations of smaller droplets.

Because they influence droplet number and size, CCN have the potential to affect cloud radiative properties (Twomey 1974; Charlson et al. 1987; Coakley

* The National Center for Atmospheric Research is sponsored by the National Science Foundation.

Corresponding author address: Dr. Cynthia H. Twohy, National Center for Atmospheric Research, P.O. Box 3000, Boulder, CO 80307-3000.

et al. 1987). For clouds with the same liquid water content and geometric thickness, those with small droplets reflect more solar radiation than those with larger droplets (Twomey 1977). A decrease in droplet size may also reduce precipitation efficiencies, thereby increasing liquid water content and extending cloud lifetimes (Albrecht 1989; Radke et al. 1989; Liou and Ou 1989).

Of particular interest is the possibility that an enhancement in CCN number would lead to an increase in the solar albedo of clouds (Twomey et al. 1984). The number of available soluble ions in a particle governs its effectiveness as a cloud condensation nucleus. Anthropogenic particles, many of which contain soluble sulfate and nitrate compounds, are often efficient CCN. Polluted clouds are likely to have more and smaller droplets and, consequently, higher albedos than pristine clouds. Therefore, anthropogenic particle emissions might have an indirect cooling effect on the earth's atmosphere. The present globally averaged value for this indirect radiative forcing has been estimated with large uncertainty at about -1 W m^{-2} , the same sign and magnitude as the direct forcing due to backscattering of solar radiation by particles (Charlson et al. 1992); these cooling influences, therefore, may be of comparable magnitude to the present warming influence (about $+2 \text{ W m}^{-2}$) of anthropogenic greenhouse gases (Hansen and Lacis 1990).

Several key mechanisms (for example, the physical and chemical controls on particle number concentration, the efficiency with which particles are incorporated as CCN, the factors affecting liquid water path, and the influence of CCN number on drizzle production and cloud lifetime) need to be better understood to establish a definitive and quantitative relationship between enhanced pollution and atmospheric cooling effects. Field studies that examine this problem have been limited, and the physical and chemical complexity of the system renders modeling attempts arduous and often inadequate; as a result, CCN-cloud interactions are usually neglected in global climate models (Twomey 1991).

2. Prior studies

Twomey et al. (1984) calculated that the light-scattering influence of anthropogenic particles, enhanced by incorporation into cloud droplets, would ultimately dominate over light-absorbing tendencies, and measurements have indicated that light absorption by particles within droplets is relatively small (Twohy et al. 1989). Cooling at the earth's surface caused by an increased number of cloud condensation nuclei has been predicted by several researchers (Hunt 1982; Charlson et al. 1987; Grassl 1988; Wigley 1989; Slingo 1990; Kaufman et al. 1991; Charlson et al. 1992). Large uncertainties due to insufficient data are common in these studies, however. Charlson et al. (1992) stressed the

need for quantification of "the enhancement in cloud droplet number concentration, which is uncertain by at least a factor of two." Many calculations have assumed a simple proportionality between enhanced CCN and additional droplet number, yet evidence points to a more complex nonlinear relationship (Jensen and Charlson 1984; Leitch et al. 1986). The geographical and temporal distribution of existing cloud optical thickness and droplet size also needs to be considered, as these factors largely determine the susceptibility of cloud albedo to increasing CCN number (Platnick and Twomey 1994).

Aircraft measurements and satellite images have suggested that relationships between CCN number, droplet number and size, and cloud radiative properties do exist. Strong correlations between the number of cloud condensation nuclei and the number of droplets in cumulus clouds (Warner and Twomey 1967) and marine stratus clouds (Hobbs et al. 1980; Hegg et al. 1991) have been documented. Barrett et al. (1979) showed that clouds nucleated by Los Angeles smog had substantially smaller droplets than marine clouds sampled 150 km upwind of the city. Stratus cloud reflectance at $3.7 \mu\text{m}$ was shown to be anticorrelated with droplet size by Durkee (1989); Kim and Cess (1993) found enhanced satellite-derived cloud albedo near coastal boundaries; and Durkee (1990) showed that zonally averaged cloud reflectances in the Northern Hemisphere are higher than those in the Southern Hemisphere. Coakley et al. (1987) observed augmented reflectance of marine stratus clouds that were apparently modified by the emissions of ships (ship tracks). Measurements made within a ship track verified an increase in particle number, a decrease in mean droplet size, and an increase in the cloud optical thickness at a visible wavelength (Radke et al. 1989; King et al. 1993).

Despite these efforts, few experiments have investigated simultaneously all the links comprising the chain between aerosol populations and cloud radiative properties. The scientific goal of this work was to observe potential relationships between pollution aerosols, droplet size, and cloud radiative characteristics through in situ aircraft and satellite measurements. Chemical and streamline analyses were also employed to help identify sources of enhanced particle number concentrations.

3. Methodology

As aerosol particle concentrations increase, droplet number concentrations are expected to eventually level off due to competition for available water vapor. The ideal environment in which to investigate the effect of increasing particle number on cloud reflectance would therefore be one where background levels of aerosol particles and droplets are low but transient sources of additional particles can perturb the background state.

The clouds should be relatively homogeneous in large-scale structure over the time and length scales of the observations, so that changes in droplet number and size due to aerosol effects can be distinguished from the effects of dynamical and thermodynamical processes. Marine stratus clouds cover 34% of the ocean surface on average (Warren et al. 1988), they often flank continental coastlines, and their albedos are very susceptible to changes in droplet size and number (Charlson et al. 1987). Consequently, they are especially appropriate for a study of this type.

Stratiform clouds over the northeastern Pacific Ocean were sampled during September and October 1989 with the National Center for Atmospheric Research (NCAR) King Air aircraft. During these months in this region, airflow streamlines can range from directly onshore, without contact with land for many days, to predominately offshore, with intrusion of polluted air from the Los Angeles and San Francisco areas. This geographical site therefore provided a range of conditions ideal for studying the influence of pollution aerosols on the stratus deck. The mobile sampling platform allowed us to reach areas of interest seen on satellite images and to conduct vertical soundings for full characterization of cloud and aerosol properties.

The aircraft was deployed from Monterey, California, when stratiform clouds were visible from satellite images and accessible from the field site. Patterns consisted of flight legs within the visually densest part of the cloud; the length of each leg was up to 300 km in horizontal extent so sufficient samples could be obtained for various chemical analyses. Mean liquid water contents calculated from droplet size distributions measured by a Particle Measurement Systems (PMS) forward scattering spectrometer probe (FSSP-100) for legs on 13 flights ranged from 0.1 to 0.3 g m⁻³, while mean droplet concentrations ranged from 50 to 800 cm⁻³. The structure of the cloud layer and the air above the marine boundary layer was documented with periodic vertical soundings. The above-cloud layer can be an important source of CCN (Paluch et al. 1992; Kawa and Pearson 1989), which may be produced photochemically (Hegg et al. 1991) or may be associated with pollution advected from the shoreline (Hudson and Frisbie 1991).

Two cases, one on 5 October 1989 and one on 26 September 1989, are presented in detail here. The 5 October cloud, formed during offshore flow conditions, exhibited interesting variations in droplet microphysics that were apparently associated with pollution; also, the overpass of the satellite containing the Advanced Very High Resolution Radiometer (AVHRR) was coincident with the flight observations. The cloud sampled during onshore flow on 26 September had very different microphysical, chemical, and optical properties from the 5 October case and provided an interesting contrast. The clouds sampled on the other days were all somewhat polluted based on the in situ

measurements; however, they are not explored further here because corresponding satellite data were not necessarily available, and microphysical variations were not as great as on 5 October.

4. Instrumentation

Temperature, pressure, humidity, air motions, and broadband irradiances are measured routinely on NCAR research aircraft. Particle and droplet measurements were also obtained using four PMS optical probes, mounted below the wingtips, that spanned size ranges from about 0.1 to 6000 μm in diameter. Direct measurements of cloud condensation nuclei (e.g., Hudson and Frisbie 1991) were not available; therefore, the PMS active scattering aerosol spectrometer probe (ASASP-100), which optically measures aerosol particle size, was used to approximate the number of accumulation (0.1–1.0 μm) and coarse-mode (>1 μm) particles that could potentially act as cloud condensation nuclei. The nominal size range of this probe specified by PMS, 0.12–3.0- μm diameter, was used for the size distributions shown later. Although the lower detection limit may be closer to 0.18- μm diameter for nonspherical salt particles (Liu et al. 1992), this will not affect our conclusions. Within clouds, the ASASP provides some information about interstitial particle distributions, although the evaporation rate of hydrated particles and the fate of cloud droplets entering the heated inlet of the instrument is not well understood (Strapp et al. 1992). The cloud-droplet size distribution was measured with the PMS FSSP-100, with sizing corrected for airspeed effects (Dye and Baumgardner 1984). Estimated root-sum-squared uncertainty is about 54% (20% precision error and 50% bias error) for FSSP concentration measurements and about 41% (18% precision error and 37% bias error) for droplet sizing if airspeed corrections are made (Baumgardner et al. 1990). The precision error is most applicable in comparing characteristics of size distributions measured by the same FSSP, but both errors are important in comparing the FSSP measurements with droplet sizes inferred from the AVHRR data. Cloud water was collected on the aircraft with a modified Mohnen slot-rod collector (Huebert and Baumgardner 1985) and analyzed by ion chromatography at the University of Rhode Island.

These measurement capabilities were supplemented with a counterflow virtual impactor (CVI). This instrument samples only droplets larger than a certain size threshold, evaporates components of the droplets that are volatile at about 323 K, and measures the residual nonvolatile components (Ogren et al. 1985; Noone et al. 1988; Twohy 1992). Aerosol particles not associated with droplets are rejected quite efficiently via a counterflow airstream out the tip; the flux of particles impinging on the tip divided by the flux of particles entering the probe is typically on the order of

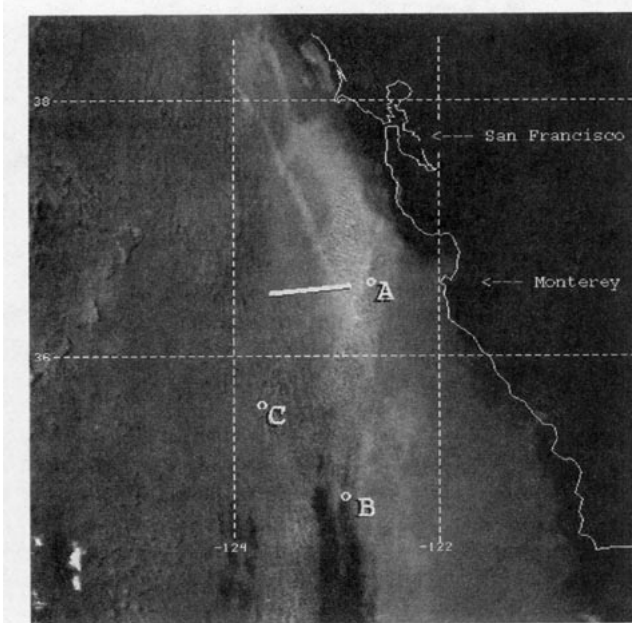


FIG. 1. AVHRR image showing cloud reflectance at $3.7 \mu\text{m}$ on 5 October 1989 (1650 UTC). Shown in white is the portion of the aircraft flight track where simultaneous microphysical measurements are presented in Fig. 3. Vertical profiles (Fig. 5) were made at points labeled A, B, and C.

10^6 . Residual particles collected downstream of the CVI include the nonvolatile portion of the CCN on which the sampled droplets formed, as well as any material gained subsequent to formation by chemical reactions, coagulation, or coalescence. These residual particles provide information about the droplets' history and will be called "droplet nuclei" here for simplicity. Downstream of the CVI, the number concentration of droplet nuclei was measured with a TSI condensation nucleus counter (CNC) and the size distribution was measured with a Climet optical particle counter (OPC).

5. Results

a. 5 October case

On 5 October 1989, the aircraft flew 150 km west from Monterey before turning to begin flight legs that approximately paralleled the coastline. Sampling on this day coincided with the passage over the area of the National Oceanic and Atmospheric Administration *NOAA-10* satellite, which carried the AVHRR. The AVHRR provides radiance data at a variety of wavelengths, the $3.7\text{-}\mu\text{m}$ signal being of special interest because it varies primarily with droplet size for clouds with liquid water paths greater than about 30 g m^{-2} (Mineart 1988; Durkee 1989). Unfortunately, AVHRR images were not able to be processed until after the experiment, so interesting features (such as ship tracks) apparent in the $3.7\text{-}\mu\text{m}$ images were not always reliably

intercepted by the aircraft flights. GOES (Geostationary Operational Environmental Satellite) satellite data were available in real-time at the Naval Postgraduate School in Monterey.

The thermal emission from the AVHRR measurements at $11 \mu\text{m}$ was used to remove emission from the radiance signal at $3.7 \mu\text{m}$, with correction for anisotropy (Mineart 1988). The $3.7\text{-}\mu\text{m}$ reflectance values reported here were taken from clouds that were analyzed as optically thick from the $0.63\text{-}\mu\text{m}$ imagery, so unit emissivity at $11 \mu\text{m}$ was assumed. Water vapor absorption above the marine boundary layer was taken to be negligible at both wavelengths, since these days were influenced by the subsidence associated with a subtropical high pressure system. The delta-Eddington approximation for multiple scattering in clouds (Joseph et al. 1976) was used to solve the radiative transfer equation for droplet size estimates.

The cloud reflectance at $3.7 \mu\text{m}$ derived for 5 October is shown in Fig. 1. A linear feature that appears to be a ship track is visible near the top of the picture. The aircraft flew near the south end of this feature, where it becomes nearly indistinguishable from the highly reflective cloud in the same location. Surface streamline analysis (Fig. 2) indicated that the mean flow near the surface was from the north-northeast, meaning that the boundary layer clouds near shore were likely to be influenced by air from the urban San Francisco Bay area.

We focus here on the portion of the flight track shown in white in Fig. 1. The $3.7\text{-}\mu\text{m}$ cloud reflectance at 1650 UTC and the microphysical properties measured from the aircraft between 1648 and 1658 UTC are shown in Fig. 3. These parameters were averaged over 1.4-km intervals to correspond to the satellite data and are plotted against distance west along the flight track. The easternmost point displayed is where the

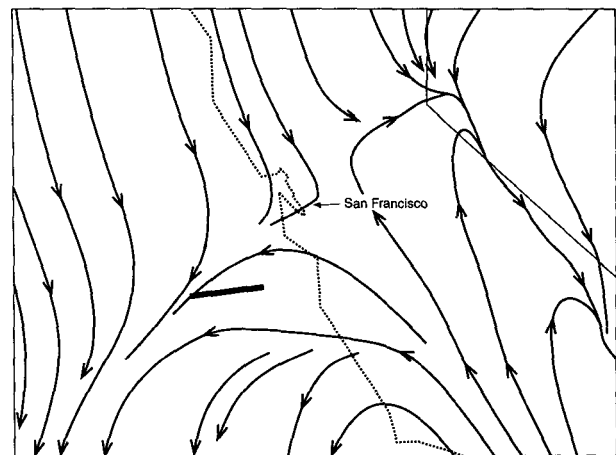


FIG. 2. Surface streamline analysis for 5 October 1989 at 1700 UTC. Flight track (heavy line) is superimposed.

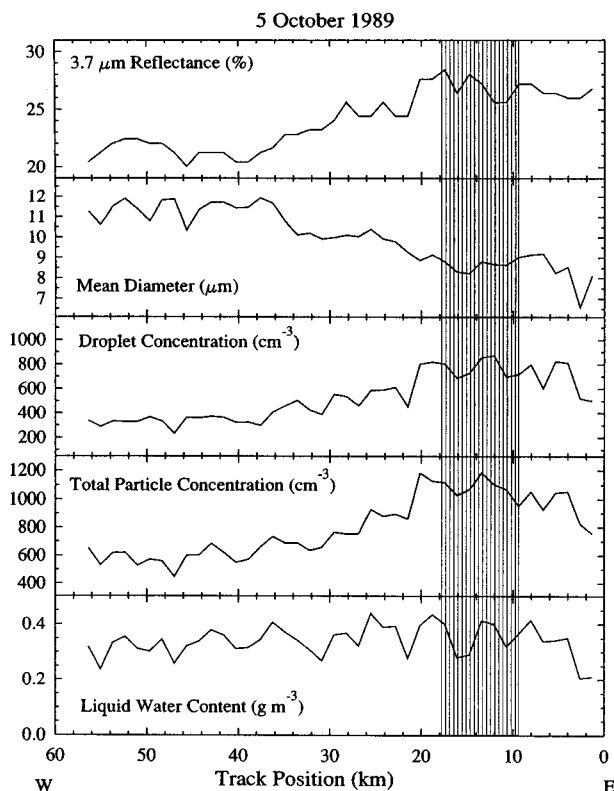


FIG. 3. Various properties of the cloud sampled on 5 October as a function of distance west along the white portion of the flight track shown in Fig. 1. Shaded area represents estimated collocation of flight track with ship track feature.

aircraft first descended into the cloud about 90 km from the shoreline.

Droplet number concentration decreased, and the mean cloud droplet size (calculated from the number of droplets measured by the FSSP in each size channel) increased as the aircraft traveled westward along the track. The satellite-derived 3.7- μm reflectance, which decreased from a value of about 27% along the east end of the track to about 20% at the west end, was anticorrelated with the mean droplet size. The collocation of the ship track feature and the flight track was estimated by extending the edges of the feature in Fig. 1 south across the flight track location. The shading represents the area of crossover (± 2 km) near the east end of the track; it corresponds to a region of slightly higher particle concentration and 3.7- μm reflectance. The near obscuration of the ship track feature in the already reflective region of cloud is consistent with the expected nonlinearity of the relationship between enhanced particle concentration and cloud microphysical response—with increasing particle number concentrations, competition for water vapor prevents nucleation of all particles and the mean droplet size will asymptotically approach a lower limit.

Also plotted in Fig. 3 is “total” particle number concentration N_T , derived by adding the number of particles measured by the FSSP to the number measured by the ASASP. This may differ from the true total particulate concentration because particles smaller than those measured by the ASASP are not included; additionally, smaller cloud droplets are likely to be measured by both the ASASP and the FSSP (Strapp et al. 1992). Total particle number concentration N_T does, however, provide a relative measure of the number of particles present within the cloud, and it is apparent that the number concentration of these particles decreased with increasing distance from the shore.

The final trace shown in Fig. 3 is liquid water content (in droplets 2 to 50 μm in diameter) derived from the FSSP data. Radke et al. (1989) observed that while droplet size decreased in a shiptrack, liquid water content increased and hypothesized that drizzle was suppressed within the shiptrack due to the absence of large droplets. Our data show that liquid water content varied little from the east to west end of the track. This does not contradict the results of the earlier study, however, because even the largest droplets we sampled (at the west end of the track) were small compared to those sampled by Radke et al. (1989) in the cleaner environment around the ship track. Significant drizzle [defined by Albrecht (1989) to occur when the mean drop diameter measured by the PMS 260-X probe was greater than 200 μm] was virtually absent all along the track sampled on 5 October. Therefore, we would not expect lower liquid water contents outside of the ship track. The relatively constant liquid water content and vertical velocity (not shown) lends credence to the hypothesis that differences in particle number concentration, not cloud dynamics, were primarily responsible for the variations in droplet number, droplet size, and ultimately, cloud reflectance that were observed.

Figure 4 shows that the satellite-derived reflectance was anticorrelated with mean droplet diameter (Fig. 4a; solid circles) and, as predicted, correlated with N_T (Fig. 4b) along the flight track. Also plotted in Fig. 4a are model-calculated reflectances at 3.7 μm from Minieart (1988) for a droplet distribution that closely resembles the average distribution measured on 5 October. The droplet size distribution used in the calculations is based on a modified gamma distribution, as described in the figure caption. The Minieart (1988) results were presented in terms of modal droplet size rather than the mean droplet size we used for the measurements. The data points in Fig. 4a associated with the calculations therefore apply to modal droplet diameters, while the experimental points represent mean droplet diameters. The slope of the measured data points is represented well by the modeled curve, but the model overestimates droplet diameters corresponding to the measured reflectances by about 2 μm . Also, mean diameters for the calculated distributions were actually larger than the modal diameters by about

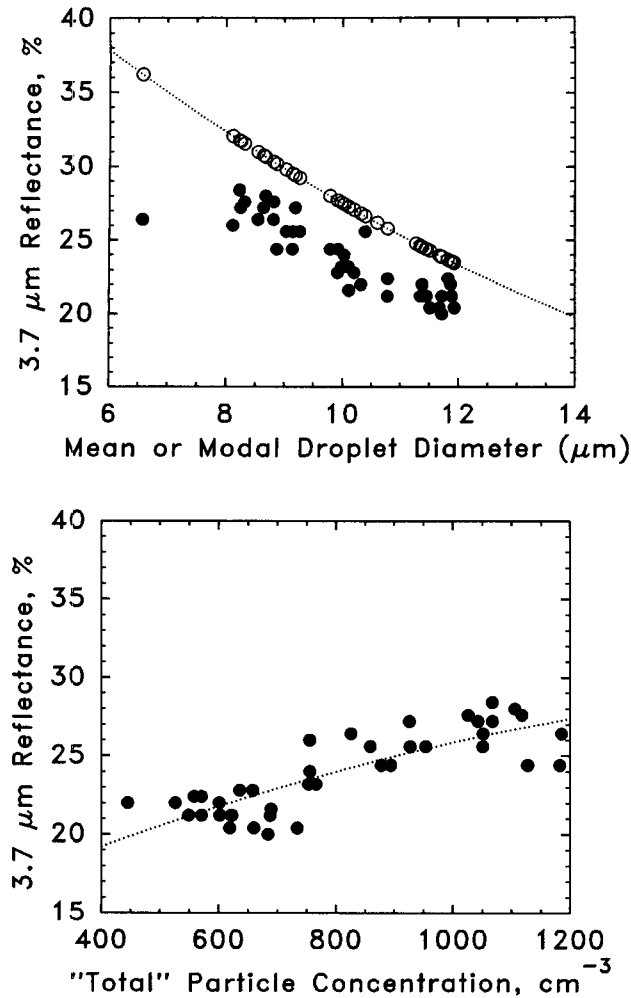


FIG. 4. (a) Reflectance at $3.7 \mu\text{m}$ as a function of mean or modal droplet diameter. Solid circles are measured values using the mean droplet diameter. Open circles were taken from Mineraert (1988) and use modal droplet diameters for a droplet size distribution based on a modified gamma distribution, $n(r) = Ar^\alpha \exp[-(\alpha/\gamma)(r/r_c)^\gamma]$, with n being droplet number, r droplet radius, and r_c modal droplet radius; A affects the amplitude of the distribution and varies with modal droplet diameter. Values of α and γ are 5.0 and 1.30. The dispersion, or standard deviation divided by mean diameter, was about 0.35 for the size distribution used by Mineraert and 0.34 for the average measured distribution; liquid water content was 0.40 g m^{-3} for the Mineraert distribution and 0.34 g m^{-3} for the measured distribution. (b) Integrated particle number concentration from the FSSP and the ASASP vs AVHRR-derived reflectance at $3.7 \mu\text{m}$.

$2 \mu\text{m}$, so the difference between measured and calculated results is actually about $4\text{-}\mu\text{m}$ diameter. This overestimate of droplet size calculated from remote sensing techniques is common to several prior studies, as discussed by Nakajima et al. (1991) and Platnick and Twomey (1994). Worth noting, however, is that in situ measurements using the FSSP data without correcting for airspeed as we did would have resulted in measured mean diameters about $1.5 \mu\text{m}$ smaller, accentuating the difference between measurements and

calculations. Also, the current difference between the measurements and calculations is, for many of the data points, within the 41% uncertainty estimated for FSSP sizing.

The dependence of $3.7\text{-}\mu\text{m}$ reflectance on droplet size predominates when the clouds have sufficient liquid water paths (vertically integrated liquid water content) for them to be opaque at this wavelength. Decreases in reflectance at $3.7 \mu\text{m}$ for liquid water paths (LWPs) less than 40 g m^{-2} were estimated from Table 6 of Mineraert (1988) to be about 0.5% at 30 g m^{-2} , 6% at 20 g m^{-2} , and 27% at 10 g m^{-2} . From the flight observations, we estimate the average LWP on 5 October to be 40 g m^{-2} , and the average optical thickness to be about 10 [using Eq. (7) of Stephens (1978) with an extinction efficiency of 2 and effective droplet radius of $5.95 \mu\text{m}$]. However, variations in both liquid water content and cloud thickness were observed. The outlying point in Fig. 4a at about $7\text{-}\mu\text{m}$ mean diameter probably represents an optically thin region (observable in data taken near the east end of the flight track in Fig. 3) where the $3.7\text{-}\mu\text{m}$ reflectance was dependent on liquid water path as well as droplet size.

Points marked A, B, and C in Fig. 1 are locations where vertical soundings were made through the above-cloud layer. Clouds observed at point A, nearest the shore, had the highest reflectance at $3.7 \mu\text{m}$ of the three sounding locations. Particle concentration measured by the ASASP at point A is depicted in Fig. 5. A layer of aerosol particles is apparent just above the

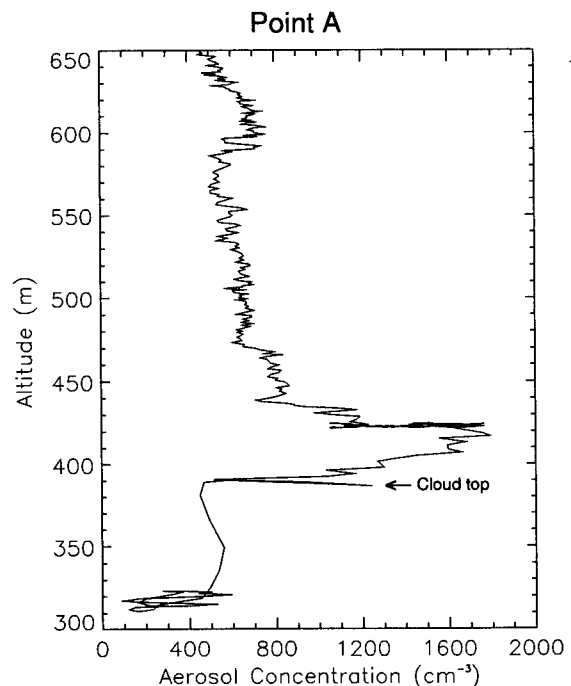


FIG. 5. Vertical profiles of aerosol particle concentration measured by the ASASP at point A (location of this point is shown in Fig. 1).

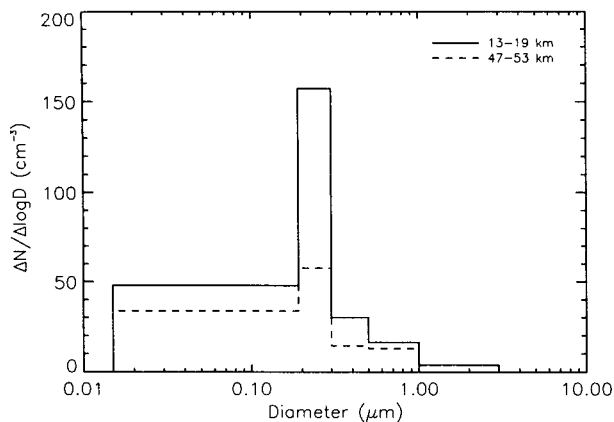


FIG. 6. Size distributions of droplet nuclei collected by the CVI in the brighter portion of the cloud near shore, 13–19 km along the flight track (solid line), and in the less reflective portion of cloud farther from shore, 47–53 km along the track (dashed line).

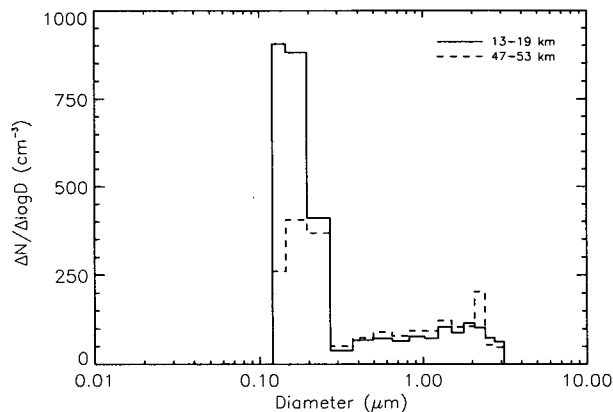


FIG. 7. Particle size distributions measured by the ASASP in the brighter portion of the cloud near shore, 13–19 km along the flight track (solid line), and in the less reflective portion of cloud farther from shore, 47–53 km along the track (dashed line).

cloud top, with peak concentrations reaching about 1800 cm^{-3} . An aerosol layer was also observed above cloud top at point B, but the peak concentrations had dropped to only about 800 cm^{-3} . Point C, offshore in the least reflective portion of the cloud, had aerosol concentrations of only about 400 cm^{-3} above cloud top. Concentrations of 400 cm^{-3} are still higher than those expected in a clean marine environment and suggest that particles can be transported above the marine boundary layer for substantial distances. These observations are consistent with those of Hudson and Frisbie (1991), who attributed aerosol layers above the stratus deck in the northeastern Pacific to pollution advected from the California coastline. The city of San Francisco was nearly 300 km upwind of point C; at the mean wind speed of 4 m s^{-1} just above the boundary layer, this corresponds to a particle residence time of about 20 h. Actual residence times may have been longer, however, due to the diurnal circulation in this region (Banta et al. 1993).

Residual nuclei from droplets larger than about $8 \mu\text{m}$ in diameter were collected by the CVI in air that was dried below 50% relative humidity. One-minute-averaged size distributions of the droplet nuclei from two different portions of the 5 October track are shown in Fig. 6. The particle size distribution represented by the solid line was taken at the near-shore end of the track in the portion of the cloud with relatively small droplets. In contrast, the distribution depicted by the dashed line originated from droplets at the west end of the flight track where the droplets were larger. The minimum size limit of the OPC used to derive the upper four channels of the distributions was $0.19\text{-}\mu\text{m}$ diameter, but a CNC was also used to measure the total number of droplet nuclei larger than $0.013 \mu\text{m}$. Data in the first size range ($0.013\text{--}0.19 \mu\text{m}$) of the distributions shown in Fig. 6 were derived by subtracting the number of particles measured by the OPC from

the number of particles measured by the CNC. The first channel of the depicted distributions is therefore quite wide, but with our knowledge of particle size distributions and data from previous experiments of this type, we expect that most of these particles actually had sizes nearer to $0.19 \mu\text{m}$ than to $0.01 \mu\text{m}$.

Figure 6 shows that there were substantially more particles forming droplets near shore than farther from shore, which is consistent with the FSSP droplet concentrations. Also, a substantial percentage of the additional droplet nuclei in the near-shore region were between 0.19 and $1.0 \mu\text{m}$ in diameter, indicative of a somewhat aged accumulation-mode aerosol (Whitby 1978).

Figure 7 shows the ASASP size distributions from the same regions of the stratus cloud (near shore: solid; offshore: dashed). These may be loosely described as “interstitial” particle distributions, although the small-

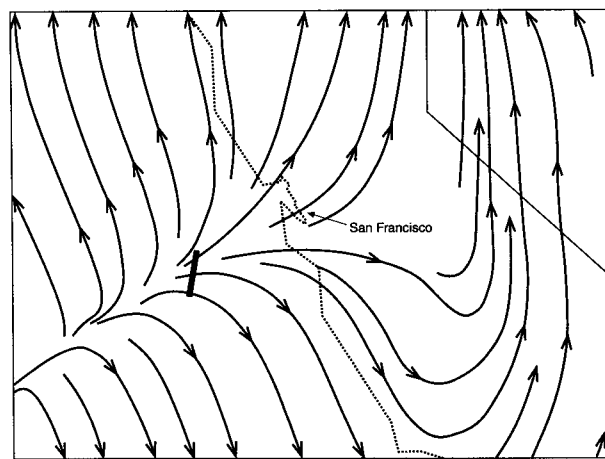


FIG. 8. Surface streamline analysis for 26 September 1989 at 1900 UTC. Flight track (heavy line) is superimposed.

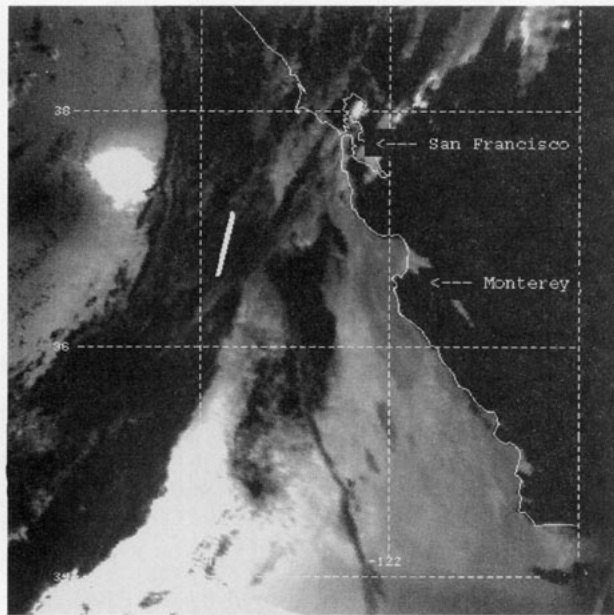


FIG. 9. AVHRR image showing cloud reflectance at $3.7 \mu\text{m}$ on 26 September 1989 (1700 UTC). Shown in white is the portion of the aircraft flight track corresponding to microphysical measurements presented in Fig. 10.

est interstitial particles were probably not detected by the ASASP. Also, it is likely that the bump on the large particle end of the size distributions represents not interstitial particles but partially evaporated or shattered cloud droplets. Despite these shortcomings, it is apparent from Fig. 7 that there were substantially more interstitial particles in the near-shore cloud. Most of these additional particles were smaller than $0.20 \mu\text{m}$ in diameter, as particles larger than this were preferentially incorporated into droplets (Fig. 6).

Particulate sulfate mass is a commonly measured quantity, so the particle mass along the flight track was derived from the ASASP (interstitial) and the CVI (in cloud) size distributions. A particle density of 1.8 g cm^{-3} was assumed, and only particles smaller than $1 \mu\text{m}$ in diameter were included in the calculations. At the east end of the track where droplet concentrations were about 800 cm^{-3} , submicron particle mass averaged about $10.5 \mu\text{g m}^{-3}$, and at the west end of the track where droplet concentrations were about 300 cm^{-3} , submicron particle mass averaged about $4.9 \mu\text{g m}^{-3}$. Based on longer-duration cloud water samples, at least half of the submicron mass is likely to be composed of sulfate. These calculations are estimated to have a root-sum-squared uncertainty of 50%.

b. 26 September case

On 26 September 1989, a frontal stratiform cloud was sampled approximately 110 km from shore. In contrast to the previous case, the surface-level flow on

this day was from the west (Fig. 8). This cloud also had the lowest droplet concentrations observed throughout the project, and the cloud microphysical and chemical properties indicated that it was quite pristine.

Figure 9 portrays the $3.7\text{-}\mu\text{m}$ reflectance derived from the NOAA-10 AVHRR data for 26 September. In this case, the satellite overpass at 1700 UTC preceded the aircraft observations by 2.7 h. Examination of the GOES visible images for 1501–2101 UTC indicated that although the cloud system moved eastward, its large-scale structure changed little during this time period. The flight track was superimposed on the satellite image with the assumption that during the 2.7-h interval the cloud system moved with the wind speed and direction actually measured within the cloud by the aircraft. The numerical AVHRR data and corresponding microphysical data taken from the aircraft near the leading edge of the cloud system's upper layer are presented in Fig. 10. Here, because the flight tracks had a north–south orientation, the distance from the south to the north end of the track is plotted on the abscissa. Although the timing differential meant we could not be certain that the satellite data accurately represent the exact portion of cloud sampled by the aircraft or how the cloud properties of interest changed between the two time intervals (cf., Minnis et al. 1992), there are general similarities in how the two types of

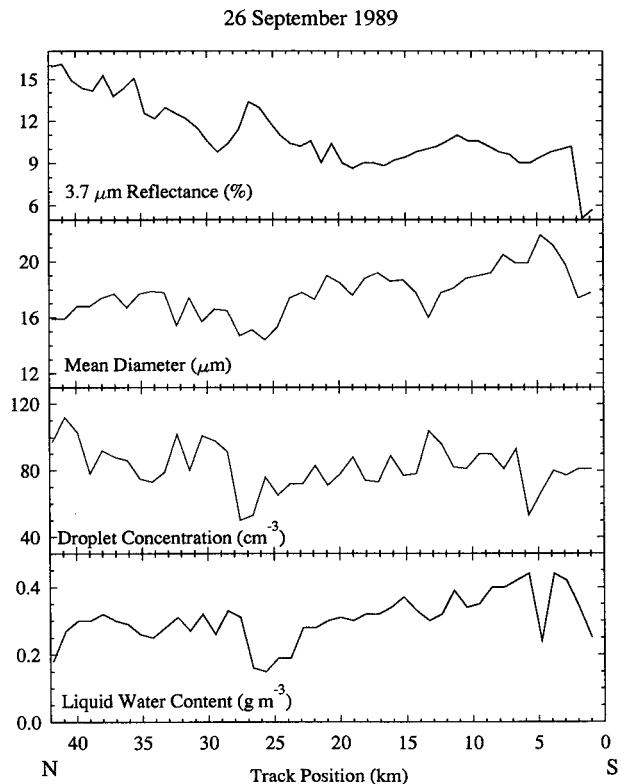


FIG. 10. Various properties of the cloud sampled on 26 September as a function of distance north along the flight track.

data vary from north to south. Perhaps more interesting, however, is a comparison of the cloud characteristics observed on this day with those observed on 5 October.

First, the satellite-derived reflectance at $3.7 \mu\text{m}$ was much lower on 26 September than on 5 October; the mean reflectance along the track on 5 October was about 23%, while on 26 September it was only 12%. Although liquid water contents were similar in both clouds, their droplet number concentration and size distributions were strikingly different. Droplet concentrations on 5 October ranged from 300 to 800 cm^{-3} , but were only about $50\text{--}100 \text{ cm}^{-3}$ on 26 September. In contrast to 5 October, there was significant drizzle present on 26 September across 6% of the cloud's horizontal extent. While the mean cloud droplet diameter for the 5 October case was approximately $10 \mu\text{m}$, it was $18 \mu\text{m}$ on 26 September, with surface-area-weighted effective diameters of 12 and $21 \mu\text{m}$, respectively. The mean and effective droplet diameters and the plotted liquid water content for 26 September may actually be underestimated slightly; since the FSSP was set on the $1\text{--}30\text{-}\mu\text{m}$ size range for this day, neither cloud droplets larger than $30 \mu\text{m}$ nor drizzle-sized drops measured by the 260-X were included when calculating these microphysical parameters.

The dissimilar character of the two clouds was also evident in their chemical composition. Concentrations of sulfate and nitrate ion measured near the west end of the flight track on 5 October and in the frontal stratus cloud on 26 September are shown in Fig. 11. Ionic equivalents per volume of cloudy air were calculated by dividing the equivalents collected (after blank subtraction) by the volume of air swept out by the rods in the same time period. This quantity is directly comparable to measurements of particulate concentrations made by others (e.g., Leitch et al. 1992, Tables 3 and 4), although it represents only the solute incorporated

into cloud droplets and not the total particulate loading.

The sulfate concentration in cloud water sampled on 5 October was higher by about an order of magnitude than the 26 September concentration. The 5 October value is also higher than sulfate aerosol concentrations measured by other researchers at remote locations (Leitch et al. 1992), despite the fact that not all aerosol particles were incorporated into cloud droplets. The cloud water sulfate concentration measured on 26 September is indicative of much cleaner air. Nitrate, which can also be associated with pollution, was nearly twice as high on 5 October as on 26 September. These chemical data support our hypothesis that urban pollution modified the clouds on 5 October and was primarily responsible for the large droplet concentrations and high reflectances observed at $3.7 \mu\text{m}$.

c. Discussion

Cloud reflectance at $3.7 \mu\text{m}$ is dominated by droplet-size effects, as discussed earlier and as corroborated by our data. Climatic impacts, however, will be most dependent on changes in cloud reflectance at visible wavelengths, where the majority of the energy in the solar spectrum is concentrated. The clouds sampled on 5 October and 26 September, while exhibiting very different chemical and microphysical characteristics, had approximately the same AVHRR-derived reflectance at $0.63 \mu\text{m}$ (48% and 50%, respectively). Reflectance at visible wavelengths is strongly dependent on liquid water path as well as droplet size. The frontal cloud sampled on the 26 September was composed of two layers, each almost 200 m deep, and therefore had a larger liquid water path (about 120 g m^{-2} vs 40 g m^{-2}) than the cloud of 5 October, which was less than 200 m deep.

Estimates of the effects of increased CCN on cloud reflectance (e.g., Charlson et al. 1987; Leitch et al. 1992) generally assume liquid water path to be invariant as droplet size changes. In situ measurements, however, have indicated that liquid water path can be either positively or negatively correlated with droplet size, depending on cloud optical thickness (Rawlins and Foot 1990; Nakajima et al. 1991). Cloud cover over the oceans can be influenced by synoptic activity, sea surface temperature (Norris and Leovy 1994) and biological activity (Falkowski et al. 1992; Parungo and Hicks 1993) as well as by anthropogenic pollution. Thus, natural variations of cloud microphysics and optical thickness must be considered when assessing the impact of increased particle loadings on cloud reflectance.

Any significant increase in cloud lifetime resulting from drizzle suppression by increased CCN would have a potentially large climatic impact. The visible reflectance of the ocean surface (about 0.07) is much smaller

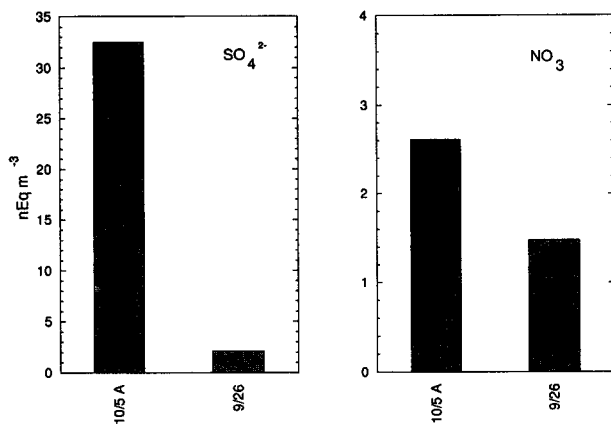


FIG. 11. Sulfate and nitrate (presented as equivalents per unit volume of cloudy air) in bulk cloud water samples on 5 October (west of point A) and on 26 September 1989.

than typical stratus and stratocumulus cloud-top visible reflectances of 0.28–0.72 (Charlson et al. 1987). The difference between the reflectance of the ocean surface and those of typical stratiform clouds therefore ranges between 0.21 and 0.65, while the maximum increase in cloud reflectance for an eightfold increase in droplet number density and constant liquid water path is only 0.16 (Charlson et al. 1987). However, quantification of any effect drizzle has on cloud lifetime is difficult without more in situ measurements and a better understanding of the natural variations in cloud microphysics.

7. Conclusions

In situ observations of aerosol particle and cloud properties off the coast of California were integrated with high-resolution satellite measurements to determine if, and under what conditions, these quantities were related. Our results are summarized below.

During offshore flow conditions on 5 October 1989, particle and droplet number concentrations increased, droplet size decreased, and satellite-derived reflectance increased coherently with increasing proximity to land. The trend in droplet size was reproduced from the AVHRR-derived reflectance at 3.7 μm , although the predicted magnitudes of droplet sizes were slightly larger than those measured by the FSSP. The location of aerosol layers above cloud, particle distributions within cloud, and the chemical composition of the cloud water supported the hypothesis that anthropogenic pollution was the primary source of the enhanced aerosol populations. The cloud microphysical properties sampled as far as 300 km downwind of San Francisco were apparently influenced by pollution aerosols. Aerosol layers just above cloud top were ubiquitous and are a potentially important source of CCN to the stratus deck. Ground-based measurements, therefore, may be insufficient to predict the indirect effects of aerosol particles on climate.

Frontal stratus clouds sampled during onshore flow conditions on 26 September were markedly different in chemical, microphysical, and radiative characteristics than those clouds sampled on 5 October. Relative to the polluted clouds, the pristine stratus clouds had, on average, sulfate concentrations lower by an order of magnitude, droplet number concentrations lower by a factor of 6, droplet sizes larger by a factor of 2, and 3.7- μm reflectance values that were smaller by a factor of 2. In addition, significant drizzle was present on 26 September, yet was absent in the polluted stratus clouds.

This study verifies that anthropogenic aerosol particles can have substantial effects on droplet number and size in stratus clouds on at least a regional scale. Climatic impacts will depend on cloud lifetime and liquid water path as well as droplet size, however. The influence of enhanced CCN on these quantities is less

straightforward and will require more extensive and longer-term studies.

Acknowledgments. Many thanks to Kurt Nielsen of the Naval Postgraduate School who provided the satellite data analysis and to Gangwoong Lee of the University of Rhode Island who performed the ion chromatography of the filter samples. This experiment was supported by the staff of the Research Aviation Facility and the program for visiting scientists at the National Center for Atmospheric Research, funded by the National Science Foundation.

REFERENCES

- Albrecht, B. A., 1989: Aerosols, cloud microphysics, and fractional cloudiness. *Science*, **245**, 1227–1230.
- Banta, R. M., L. D. Olivier, and D. H. Levinson, 1993: Evolution of the Monterey Bay sea-breeze layer as observed by pulsed Doppler lidar. *J. Atmos. Sci.*, **50**, 3959–3982.
- Barrett, E. W., F. P. Parungo, and R. F. Pueschel, 1979: Cloud modification by urban pollution: A physical determination. *Meteor. Rundsch.*, **32**, 136–149.
- Baumgardner, D., W. A. Cooper, and J. E. Dye, 1990: Optical and electronic limitations of the forward-scattering spectrometer probe. *Liquid Particle Size Measurement Techniques*. Vol. 2. E. D. Hirtleman, W. D. Bachalo, and Philip G. Felton, Eds., Amer. Soc. for Testing and Materials, 115–127.
- Cass, G. R., and F. H. Shair, 1984: Sulfate accumulation in a sea breeze/land breeze circulation system. *J. Geophys. Res.*, **89**, 1429–1438.
- Charlson, R. J., J. E. Lovelock, M. O. Andreae, and S. G. Warren, 1987: Oceanic phytoplankton, atmospheric sulphur, cloud albedo and climate. *Nature*, **326**, 665–661.
- , S. E. Schwartz, J. M. Hales, R. D. Cess, J. A. Coakley Jr., J. E. Hansen, and D. J. Hofmann, 1992: Climate forcing by anthropogenic aerosols. *Science*, **255**, 423–430.
- Coakley, J. A., Jr., R. L. Bernstein, and P. A. Durkee, 1987: Effect of ship-track effluents on cloud reflectivity. *Science*, **237**, 1020–1022.
- Durkee, P. A., 1989: Observations of aerosol–cloud interactions in satellite-detected visible and near-infrared radiance. Preprints, *Symp. on the Role of Clouds in Atmospheric Chemistry and Climate*, Anaheim, CA, Amer. Meteor. Soc., 157–160.
- , 1990: Global analysis of aerosol–cloud interactions: Implications for climate change processes. Preprints, *Fifth Conf. on Satellite Meteorology and Oceanography*, London, England, Amer. Meteor. Soc. and Roy. Meteor. Soc., 35–37.
- Dye, J. E., and D. Baumgardner, 1984: Evaluation of the forward scattering spectrometer probe. Part I: Electronic and optical studies. *J. Atmos. Oceanic Technol.*, **1**, 329–344.
- Falkowski, P. G., Y. Kim, Z. Kolber, C. Wilson, C. Wirick, and R. Cess, 1992: Natural versus anthropogenic factors affecting low-level cloud albedo over the North Atlantic. *Science*, **256**, 1311–1313.
- Grassl, H., 1988: What are the radiative and climatic consequences of the changing concentration of atmospheric aerosol particles? *The Changing Atmosphere*, S. Rowland and I. S. A. Isaken, Eds., Wiley, 187–199.
- Hansen, J. E., and A. A. Lacis, 1990: Sun and dust versus greenhouse gases: An assessment of their relative roles in global climate change. *Nature*, **346**, 713–719.
- Hegg, D. A., L. F. Radke, and P. V. Hobbs, 1991: Measurements of Aitken nuclei and cloud condensation nuclei in the marine atmosphere and their relation to the DMS–cloud–climate hypothesis. *J. Geophys. Res.*, **96**, 18 727–18 733.
- Hobbs, P. V., J. L. Stith, and L. F. Radke, 1980: Cloud-active nuclei from coal-fired electric power plants and their interactions with clouds. *J. Appl. Meteor.*, **19**, 439–451.

- Hudson, J. G., and P. R. Frisbie, 1991: Cloud condensation nuclei near marine stratus. *J. Geophys. Res.*, **96**, 20 795–20 808.
- Huebert, B. J., and D. Baumgardner, 1985: A preliminary evaluation of the Mohren slotted-rod cloud water collector. *Atmos. Environ.*, **19**, 843–846.
- Hunt, B. G., 1982: An investigation with a general circulation model of the climatic effects of cloud albedo changes caused by atmospheric pollution. *J. Appl. Meteor.*, **21**, 1071–1079.
- Jensen, J. B., and R. J. Charlson, 1984: On the efficiency of nucleation scavenging. *Tellus*, **34B**, 367–375.
- Joseph, J. H., W. J. Wiscombe, and J. A. Weinman, 1976: The delta-Eddington approximation for radiative flux transfer. *J. Atmos. Sci.*, **33**, 2452–2459.
- Kaufman, Y. J., R. S. Fraser, and R. L. Maloney, 1991: Fossil fuel and biomass burning effect on climate—Heating or cooling? *J. Climate*, **4**, 578–588.
- Kawa, S. R., and R. Pearson Jr., 1989: An observational study of stratocumulus entrainment and thermodynamics. *J. Atmos. Sci.*, **46**, 2649–2661.
- Kim, Y., and R. D. Cess, 1993: Effect of anthropogenic sulfate aerosols on low-level cloud albedo over oceans. *J. Geophys. Res.*, **98**, 14 883–14 885.
- King, M. D., L. F. Radke, and P. V. Hobbs, 1993: Optical properties of marine stratocumulus clouds modified by ships. *J. Geophys. Res.*, **98**, 2729–2739.
- Leitch, W. R., J. W. Strapp, G. A. Isaac, and J. G. Hudson, 1986: Cloud droplet nucleation and cloud scavenging of aerosol sulphate in polluted atmospheres. *Tellus*, **38B**, 328–344.
- , G. A. Isaac, J. W. Strapp, C. M. Banic, and H. A. Wiebe, 1992: The relationship between cloud droplet number concentrations and anthropogenic pollution: Observations and climatic implications. *J. Geophys. Res.*, **97**, 2463–2474.
- Liou, K.-N., and S.-C. Ou, 1989: The role of cloud microphysical processes in climate: An assessment from a one-dimensional perspective. *J. Geophys. Res.*, **94**, 8599–8607.
- Liu, P. S. K., W. R. Leitch, J. W. Strapp, and M. A. Wasey, 1992: Response of particle measuring systems airborne ASASP and PCASP to NaCl and latex particles. *Aerosol Sci. Technol.*, **16**, 83–95.
- Mineart, G. M., 1988: Multispectral satellite analysis of marine stratocumulus cloud microphysics. M. S. thesis, Department of Meteorology, Naval Postgraduate School, Monterey, CA, 138 pp.
- Minnis, P., P. W. Heck, D. F. Young, C. W. Fairall, and J. B. Snider, 1992: Stratocumulus cloud properties derived from simultaneous satellite and island-based instrumentation during FIRE. *J. Appl. Meteor.*, **31**, 317–339.
- Nakajima, T., M. D. King, J. D. Spinhirne, and L. F. Radke, 1991: Determination of the optical thickness and effective particle radius of clouds from reflected solar radiation measurement. Part II: Marine stratocumulus observations. *J. Atmos. Sci.*, **48**, 728–750.
- Noone, K. J., J. A. Ogren, J. Heintzenberg, R. J. Charlson, and D. S. Covert, 1988: Design and calibration of a counterflow virtual impactor for sampling of atmospheric fog and cloud droplets. *Aerosol Sci. Technol.*, **8**, 235–244.
- Norris, J. R., and C. B. Leovy, 1994: Interannual variability in stratiform cloudiness and sea surface temperature. *J. Climate*, **7**, 1915–1925.
- Ogren, J. A., J. Heintzenberg, A. Zuber, K. J. Noone, and R. J. Charlson, 1985: Measurements of the size-dependence of solute concentrations in cloud droplets. *Tellus*, **41B**, 24–31.
- Paluch, I. R., D. H. Lenschow, J. G. Hudson, and R. Pearson Jr., 1992: Transport and mixing processes in the lower troposphere over the ocean. *J. Geophys. Res.*, **97**, 7527–7541.
- Parungo, F., and B. Hicks, 1993: Sulfate aerosol distributions and cloud variations during El Niño anomalies. *J. Geophys. Res.*, **98**, 2667–2675.
- Platnick, S., and S. Twomey, 1994: Determining the susceptibility of cloud albedo to changes in droplet concentration with the Advanced Very High Resolution Radiometer. *J. Appl. Meteor.*, **33**, 334–347.
- Radke, L. F., and P. V. Hobbs, 1976: Cloud condensation nuclei on the Atlantic seaboard of the United States. *Science*, **193**, 999–1002.
- , J. A. Coakley Jr., and M. D. King, 1989: Direct and remote sensing observations of the effects of ships on clouds. *Science*, **246**, 1146–1149.
- Rawlins, F., and J. S. Foot, 1990: Remotely sensed measurements of stratocumulus properties during FIRE using the C130 aircraft multi-channel radiometer. *J. Atmos. Sci.*, **47**, 2488–2503.
- Slingo, A., 1990: Sensitivity of the earth's radiation budget to changes in low clouds. *Nature*, **343**, 49–51.
- Stephens, G. L., 1978: Radiation profiles in extended water clouds. II: Parameterization schemes. *J. Atmos. Sci.*, **35**, 2123–2132.
- Strapp, J. W., W. R. Leitch, and P. S. K. Liu, 1992: Hydrated and dried aerosol-size-distribution measurements from the particle measuring systems FSSP-300 probe and the deiced PCASP-100X probe. *J. Atmos. Oceanic Technol.*, **9**, 548–555.
- Twohy, C. H., 1992: On the size dependence of the chemical properties of cloud droplets: Exploratory studies by aircraft. The University of Washington and the National Center for Atmospheric Research, NCAR/CT-137 (Cooperative Thesis No. 137), 239 pp.
- , S. G. Warren, L. F. Radke, and R. J. Charlson, 1989: Light-absorbing material extracted from cloud droplets and its effect on cloud albedo. *J. Geophys. Res.*, **94**, 8623–8631.
- Twomey, S., 1974: Pollution and the planetary albedo. *Atmos. Environ.*, **8**, 1251–1256.
- , 1977: The influence of pollution on the shortwave albedo of clouds. *J. Atmos. Sci.*, **34**, 1149–1152.
- , 1991: Aerosols, clouds and radiation. *Atmos. Environ.*, **25A**, 2435–2442.
- , and T. A. Wojciechowski, 1969: Observations of the geographical variation of cloud nuclei. *J. Atmos. Sci.*, **26**, 684–688.
- , M. Piepgrass, and T. L. Wolfe, 1984: An assessment of the impact of pollution on global cloud albedo. *Tellus*, **36B**, 356–366.
- Warner, J., and S. Twomey, 1967: The production of cloud nuclei by cane fires and the effect on cloud droplet concentration. *J. Atmos. Sci.*, **24**, 704–706.
- Warren, S. G., C. J. Hahn, J. London, R. M. Chervin, and R. L. Jenne, 1988: Global distribution of total cloud cover and cloud type amounts over the ocean. U.S. Dept. of Energy, Washington D.C., and the National Center for Atmospheric Research, Boulder, Colorado, DOE/ER-0406 or NCAR/TN-317+STR, 212 pp.
- Whitby, K. T., 1978: The physical characteristics of sulfur aerosols. *Atmos. Environ.*, **12**, 135–159.
- Wigley, T. M. L., 1989: Possible climate change due to SO₂-derived cloud condensation nuclei. *Nature*, **339**, 365–367.